AIAA SciTech
4-8 January 2016, San Diego, California, USA
AIAA Atmospheric Flight Mechanics Conference

Rapid Indirect Trajectory Optimization of a Hypothetical Long Range Weapon System

Michael J. Grant* and Thomas Antony †
Purdue University, West Lafayette, Indiana 47907-2045

This investigation illustrates that complex, highly constrained hypersonic trajectory optimization can be performed for long range weapon systems using indirect optimization methods. It is shown that initial guesses to the optimal solutions can be effectively constructed using analytic ballistic trajectory solutions. The evolution to complex optimal trajectories from these initial guesses is made possible by overcoming the historical challenges of indirect optimization methods in a largely automated approach. The manner in which indirect mathematical information is integrated into the automated design methodology to solve this type of problem is described. Example mission design scenarios illustrate the speed of the methodology and quality of the optimal solutions to support practical aerospace conceptual design studies.

Nomenclature

H	scale height, m	r_e	Earth radius, m
k	heat rate coefficient, $\sqrt{\text{kg}}/\text{m}$	r_n	vehicle nose radius, m
L	lift force magnitude, N	t	time, s
L/D	lift to drag ratio	u	control
m	vehicle mass, kg	v	relative velocity magnitude, m/s
r	radial magnitude, m	x	state

α	angle of attack, deg	ϕ	latitude, deg
β	ballistic coefficient, kg/m^2	ψ	azimuth, deg
γ	relative flight path angle, deg	ρ	atmospheric density, kg/m^3
λ	costate	ρ_0	atmospheric density at the surface, kg/m^3
μ	gravitational parameter, m^3/s^2	σ	bank angle, deg
ω	Earth's rotation rate, rad/s	θ	longitude, deg

I. Introduction

Traditionally, the mission design of hypersonic systems is accomplished by solving the optimal control problem under a specific set of simplifying assumptions[1–3] or by using direct optimization methods.[4–12] In Refs. 2 and 3, an elaborate derivation of the necessary conditions of optimality is performed for a hypersonic cruise vehicle in which solutions are obtained for constant altitude flight with either a constant velocity or a prescribed deceleration profile. This simplified problem was used to validate the optimal solutions obtained by GPOCS. For the three dimensional trajectory optimization also performed, the covectors obtained from GPOCS were used to determine the optimal control profiles derived from the necessary conditions of optimality. Comparisons to the GPOCS optimal control history provided confidence in the quality of the GPOCS solution. In Ref. 5, it is noted that the complexities associated with solving the necessary conditions

*Assistant Professor, School of Aeronautics and Astronautics, Senior Member AIAA, mjgrant@purdue.edu
†Graduate Student, School of Aeronautics and Astronautics, Student Member AIAA, tantony@purdue.edu

as a two-point boundary value problem prevents the approach from being a viable option to generate generic footprints. To bypass these complexities without resorting to simplifying assumptions of the equations of motion, a Legendre pseudospectral method contained within the DIDO software package is used to generate footprints. Comparisons are made to optimal control solutions for a reduced order model to highlight the improved solutions obtained from DIDO. In Ref. 6, a Gauss pseudospectral method is used to generate various optimal hypersonic trajectories using the GPOPS software package. Comparisons to POST were made to highlight the improved solutions obtained using the GPOPS software. In Ref. 7, a DIDO solution to an entry problem was compared to a subset of the necessary conditions of optimality. The covectors obtained from DIDO were used to calculate the optimal controls obtained from the necessary conditions of optimality. Comparisons to the DIDO control history provided confidence in the DIDO solution. Additionally, the Hamiltonian was verified to be a near constant value of zero as required by the necessary conditions of optimality.

In all cases, the use of direct optimization methods is preferred over optimal control theory to generate complex non-simplified optimal trajectories of interest. As such, these methods serve a practical means of performing complex trajectory optimization in which portions of the necessary conditions of optimality from optimal control theory are used as a checking mechanism to verify the quality of the direct solution. The common checks that are performed consist of using the covectors to create the corresponding control and Hamiltonian values associated with optimal control theory. Comparisons to the direct control history and the expected constant Hamiltonian value of zero (for typical trajectory optimization problems) provide confidence in the quality of the direct solution. This overall solution approach is particularly appealing because it overcomes the three historical limitations that arise when solving the full optimal control problem:[13]

1. Approach requires knowledge of optimal control theory and the development of lengthy necessary conditions of optimality.

2. If the problem contains path inequalities, it is necessary to make an *a priori* estimate of the constraint-arc sequence.

3. It is difficult to provide a good initial guess, especially in costates, to converge to a solution.

Prior research by Grant has demonstrated that the historical optimal control challenges associated with indirect optimization methods can be largely overcome to perform hypersonic mission design. The creation of the necessary conditions of optimality is performed in a completely automated fashion by leveraging modern symbolic computational tools such a Mathematica. By formulating the optimality conditions in a generic fashion, the application of appropriate boundary conditions associated with various constraint arc sequences can be dynamically enforced by employing a continuation process.[14,15] Additionally, by solving a sequence of progressively difficult optimization problems via continuation, it is possible to create complex optimal trajectory solutions that fully satisfy the necessary conditions of optimality without supplying a good initial guess to the complex solution. This investigation describes the maturation of the indirect optimization methodology to construct complex, high performance, optimal trajectories associated with a theoretical long range weapon system. The corresponding advancements include:

1. Accommodation of arbitrary degrees of freedom and number of controls.

2. Incorporation of all candidate control solutions with an automated selection based on Pontryagin's Minimum Principle.

3. Dynamic scaling during the continuation process.

4. Development of necessary conditions of optimality for all possible mission scenarios of interest to the designer based on objective and constraint information.

With these advancements, a largely automated process has been developed that only requires user input of the optimization problem and algorithm settings as well as an initial guess to seed the continuation process. As such, nearly all of the indirect optimization functionality is performed transparently to the user. The manner in which these advancements were made is described below, and representative long range weapon mission design scenarios are provided to illustrate the utility of this approach to perform practical conceptual aerospace design.

II. Indirect Methodology Enhancements

A. Extension to Arbitrary Degrees of Freedom and Number of Controls

For this study, an unpowered hypersonic trajectory is optimized with environment parameters shown in Table 1. An exponential atmosphere and spherical planet are assumed. A common set of glide body deployment and target conditions is shown in Table 2. Note that these values represent fictitious but relevant mission scenarios. Both angle of attack, α, and bank angle, σ, are used as control variables in the equations of motion shown in Eqs. (1)-(6). The aerodynamics are determined from a drag polar model of a generic, slender vehicle with a mass of approximately 350 kg and a peak L/D of approximately 2.5.

Table 1. Environment parameters.

Parameter	*Value*
Scale Height, H	7500 m
Surface Density, ρ_o	1.2 kg/m^3
Gravitational Parameter, μ	3.986×10^{14} m^3/s^2
Earth Radius, r_e	6378000 m
Rotation Rate, ω	7.292×10^{-5} rad/s
Heat Rate Coefficient, k	1.742×10^{-4} $\sqrt{kg}/m$

Table 2. Glide body deployment and impact conditions.

State	*Glide Body Deployment Condition*	*Impact Condition*
Altitude, h	80,000 m	4,570 m
Velocity, v	6,000 m/s	free
Flight-Path Angle, γ	free	-60 deg
Latitude, ϕ	23.14 deg	33.66 deg
Longitude, θ	64.07 deg	67.63 deg

$$\frac{dr}{dt} = v\sin\gamma \tag{1}$$

$$\frac{d\theta}{dt} = \frac{v\cos\gamma\cos\psi}{r\cos\phi} \tag{2}$$

$$\frac{d\phi}{dt} = \frac{v\cos\gamma\sin\psi}{r} \tag{3}$$

$$\frac{dv}{dt} = -\frac{D}{m} - \frac{\mu\sin\gamma}{r^2} + \omega^2 r\cos\phi(\sin\gamma\cos\phi - \cos\gamma\sin\phi\sin\psi) \tag{4}$$

$$\frac{d\gamma}{dt} = \frac{L\cos\sigma}{mv} - \frac{\mu\cos\gamma}{vr^2} + \frac{v\cos\gamma}{r} + 2\omega\cos\phi\cos\psi + \omega^2 r\cos\phi(\cos\gamma\cos\phi + \sin\gamma\sin\phi\sin\psi) \tag{5}$$

$$\frac{d\psi}{dt} = \frac{L\sin\sigma}{mv\cos\gamma} - \frac{v\cos\gamma\cos\psi\tan\phi}{r} + 2\omega(\tan\gamma\cos\phi\sin\psi - \sin\phi) - \frac{\omega^2 r\sin\phi\cos\phi\cos\psi}{v\cos\gamma} \tag{6}$$

The use of higher-fidelity models, including tabular data, is not precluded in this methodology. Such models may require use of numerical root-solving solutions in place of the analytic root-solving solutions used in this investigation. This distinction can be determined autonomously during formulation of the necessary conditions of optimality. Note that the indirect optimization framework is capable of supporting any number of states and parameters. The necessary conditions of optimality are formulated transparently to the user, and the framework is capable of adapting to the design problem of interest.

B. Assessment of Multiple Control Options

The use of parametric aerodynamic models is particularly useful because it enables all control options to be identified during development of the necessary conditions of optimality. As such, it is beneficial to convert tabulated data into parametric form. For example, flight along a stagnation heat rate constraint requires a certain drag profile. The angle of attack is chosen to match the necessary drag profile, and for symmetric

vehicles, the same drag can be achieved with a positive or negative angle of attack notionally shown in Eq. (7). All combinations of possible control solutions in angle of attack and bank are assembled into candidate branches as shown in Table 3 for two possible solutions in angle of attack, α, and two possible solutions for bank angle, σ.

$$\begin{aligned} \alpha_1 &= f(x, \lambda) \\ \alpha_2 &= -f(x, \lambda) \end{aligned} \tag{7}$$

Table 3. Example of candidate control branches.

Branch 1	*Branch 2*	*Branch 3*	*Branch 4*
α_1	α_2	α_1	α_2
σ_1	σ_1	σ_2	σ_2

During the indirect optimization process, the proper control branch is selected based on Pontryagin's Minimum Principle as described by Eq. (8), where "*" refers to the optimal solution.[16–18] This procedure is used for both constrained and unconstrained trajectory segments, and this approach provides an additional optimality condition to rapidly identify the best trajectory among possible candidates. Since all branches are evaluated at each point in time, it is possible to transition from one control branch to another along an optimal trajectory. This control selection process is fully automated and performed transparently to the designer.

$$H(x(t)^*, u(t)^*, \lambda(t)^*, t) \leq H(x(t)^*, u(t), \lambda(t)^*, t) \tag{8}$$

C. Dynamic Scaling During The Continuation Process

The continuation methodology is particularly useful for scaling analysis. It is generally difficult to identify the appropriate scaling of time, states, costates, corner conditions, etc. for complex hypersonic solutions. By starting with a relatively simple and short optimization problem, there exists much flexibility in the choice of scaling. During the continuation process, it is possible to observe the history of solution information to determine how the previous problems should have been scaled. This information is used to determine how future optimization problems should be scaled during the continuation process. This dynamic scaling capability is fully automated and only requires the user to specify which calculations are associated with the scaling of each dimensional unit. The ability to perform this dynamic scaling enables solution convergence in the example mission scenarios provided herein.

D. Development of Necessary Conditions for All Mission Scenarios

During formulation of the necessary conditions of optimality, it is possible to impose interior point constraints (*e.g.*, waypoint constraint), path constraints (*e.g.*, stagnation point heat rate constraint), initial state constraints, terminal state constraints, etc. Path constraints are often imposed in a manner that also results in a separate set of interior point constraints at the entrance to the path constraint. As such, the algorithm is capable of generically grouping all relevant constraints in their various forms and accounting for them generically during the continuation process. This is particularly useful as the necessary conditions of optimality are algorithmically expressed in a single form, enabling easy accommodation of all possible mission scenarios that may include a subset of constraint types, various orders of constraints, etc. This ability to dynamically stitch together the necessary conditions of optimality for all possible missions scenarios is particularly useful during the continuation process in which the order of active constraints is not known *a priori*.

III. Construction of Initial Guess to Seed The Continuation Process

These advancements enable the rapid construction of very high quality indirect solutions in a largely automated manner. In the following examples, a hypothetical US warship is located near the Gulf of Oman. A hypothetical high-value target is located in a cave within a mountain range inside Afghanistan. The long range weapon must be delivered with maximum velocity to the target as described by the minimizing

cost functional shown in Eq. (9). To seed the continuation process, a relatively simple, initial optimization problem is solved that consists of the weapon traveling nearly straight down from an assumed glide body deployment location. By placing the target underneath the deployment location, the optimal solution would consist of a near-ballistic trajectory that maximizes the ballistic coefficient of the vehicle. As such, the analytic Allen and Eggers trajectory solution can be used to rapidly construct a high quality initial guess to converge to this initial solution that serves as a seed to the continuation process.[19]

$$J = -v_f^2 \tag{9}$$

Assuming the drag force dominates the gravitational force and that the flight-path angle is constant for the steep trajectory, a closed-form expression for the relationship between altitude and velocity can be constructed as shown in Eq. (10), where $C = \frac{\rho_0 H}{2\beta \sin\gamma}$ and V_0 corresponds to the initial velocity of the glide body weapon at the location of deployment. The assumptions of a constant flight-path angle and heading as well as a linearly varying latitude and longitude along the near straight down trajectory enables the construction of an initial guess for the states of the maximum terminal velocity trajectory. To prevent singularities in the equations of motion, a constant flight-path angle of -80 deg was chosen.

$$v = v_0 \exp[Ce^{-h/H}] \tag{10}$$

The corresponding costates along this trajectory can be calculated via reverse integration from the terminal point. Since this initial guess is nearly optimal, the terminal velocity costate can be computed as shown in Eq. (11). Additionally, the terminal costates in flight-path angle, latitude, longitude, and azimuth are chosen to be zero. The terminal altitude costate is calculated by noting that the Hamiltonian can be approximated as zero at the terminal point for this near-optimal trajectory.

$$\lambda_{v,f} = -2v_f \tag{11}$$

The near-ballistic initial guess is used to rapidly converge to the downward optimal trajectory shown in Fig. 1. This convergence illustrates that a sufficiently accurate initial guess can be constructed via an approximate trajectory solution without insight into the optimal costate values. With this initial downward solution, the initial conditions can be incrementally (but rapidly) changed to match the appropriate set of glide body deployment conditions in Table 2 via continuation. To ensure feasibility during this process, the target is also moved to an intermediate location towards the target of interest. After this is completed, the target is moved to the location of interest as shown in Fig. 2. At the end of this process, a maximum terminal velocity trajectory is constructed between the assumed glide body deployment location and target. It is from this final trajectory that various trade studies can also be rapidly performed via continuation to study the performance of the weapon across a range of representative mission scenarios of interest.

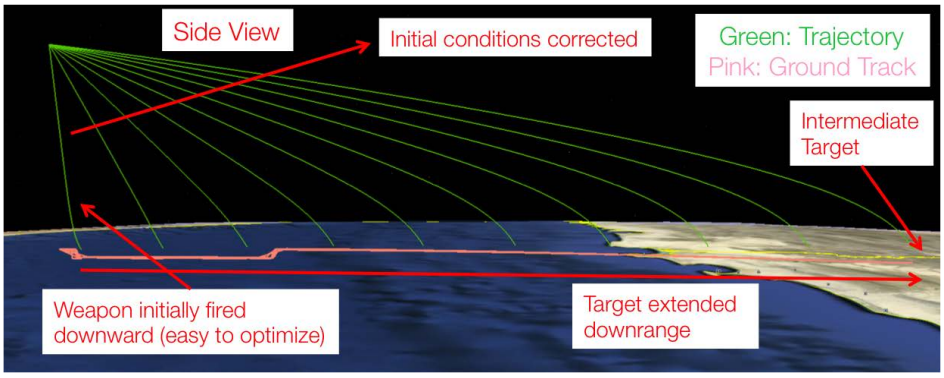

Figure 1. Initial downward optimal solution and initial condition correction.

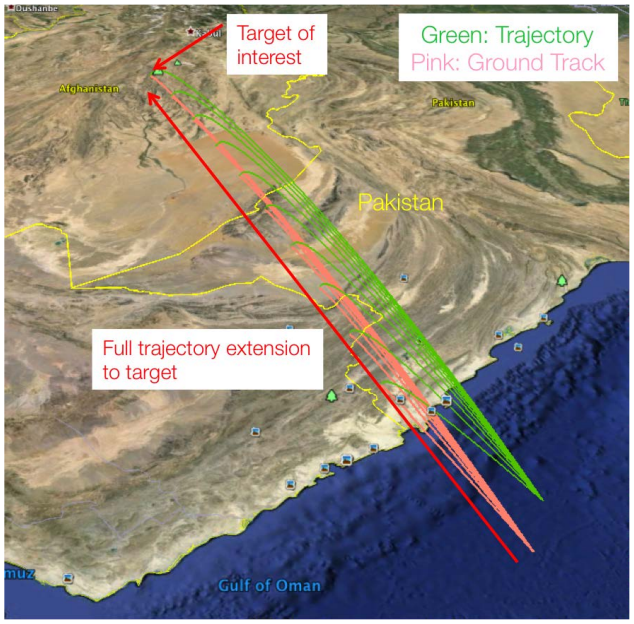

Figure 2. Extension of trajectory to target of interest.

IV. Representative Mission Scenarios

The following hypothetical mission scenarios were developed to illustrate the ability to construct high quality, complex, indirect solutions for long range weapon systems. Note that the necessary conditions of optimality are fully satisfied along the entirety of each optimal solution. To minimize execution time, the indirect optimization framework is executed on an already obsolete graphics processing unit (GPU). This enables each individual optimal solution to be constructed in a fraction of a second during the continuation process.

A. Impact Geometry Constraints at Target

This hypothetical example illustrates the application of user-specified terminal constraints in position, azimuth, and flight-path angle. In this example, the long range weapon must be delivered with maximum velocity at the appropriate impact geometries determined by the terrain and orientation of the cave entrance. As such, the terminal flight-path angle is constrained to -60 deg. To illustrate that multiple impact geometries can be rapidly satisfied, solutions for a range of terminal heading constraints are rapidly constructed using indirect methods. The full sweep of long range trajectories is shown in Fig. 3. Note that in this example, the trajectories are clustered together for the majority of the trajectory, and Fig. 4 illustrates the trajectory differences prior to impact.

In this example, a sweep of northerly-westerly-southerly terminal headings is performed. As expected, trajectories that impact in a northerly direction result in direct flight to the target. Alternatively, southerly trajectories result in flight over the target, and westerly trajectories result in banked

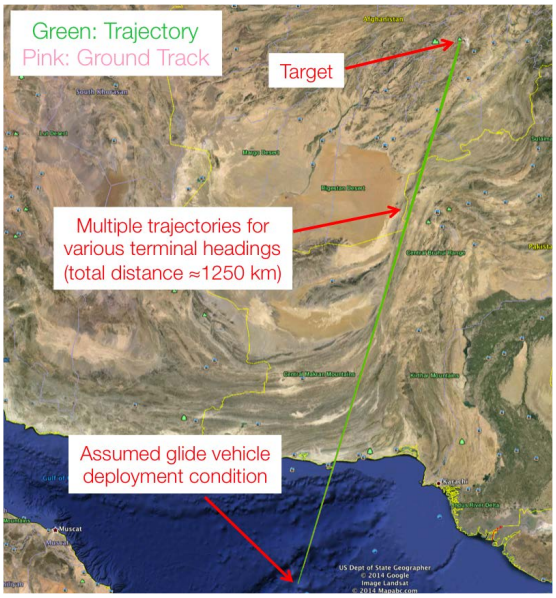

Figure 3. View of full terminal heading constrained trajectories.

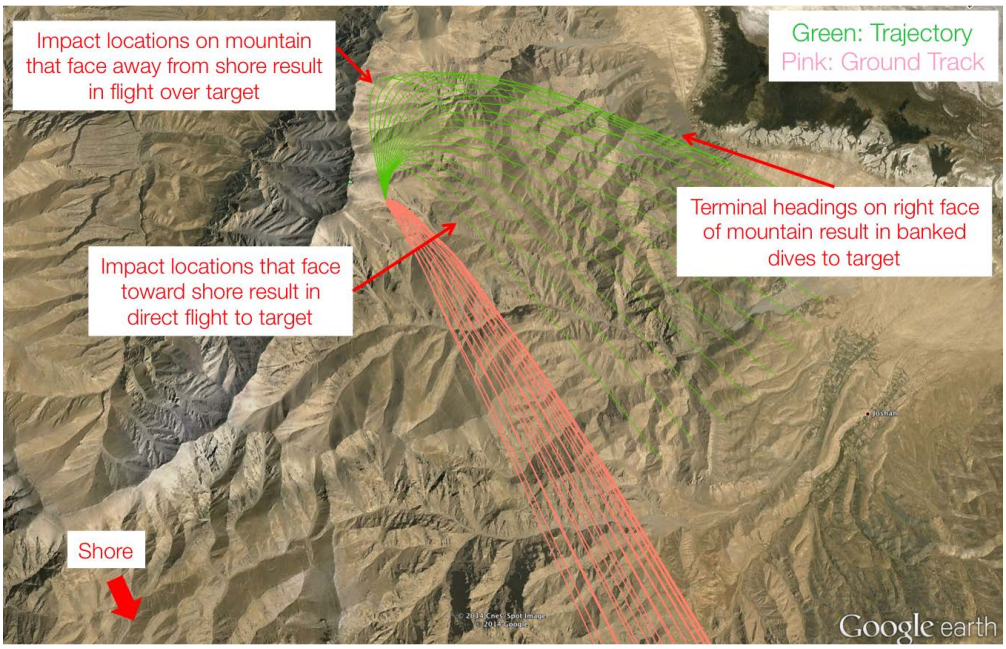

Figure 4. Pre-impact view from above-left vantage point.

dives to the target. All of these trajectories maximize terminal velocity at the target while satisfying the constraint in terminal heading. The entire set of optimal trajectories is constructed in 24 seconds using the obsolete GPU. Additionally, this process does not require any user insight of the complex optimal solutions. Since the necessary conditions of optimality are satisfied along each trajectory, the solutions are of highest quality. Fig. 5 illustrates the terminal velocity penalty associated with trajectories that have large terminal heading angles that are directed southward. During the continuation process, the optimal controls include a banked turn to target (also shown in Fig. 4) as well as an increase in angle of attack to perform more aggressive terminal maneuvers. Note that in this first example, no complex maneuvers are required to satisfy the terminal constraint. The corresponding costates shown in Fig. 6 are also well behaved. Note that the longitude costate is constant as expected due to the independence of the equations of motion from longitude.

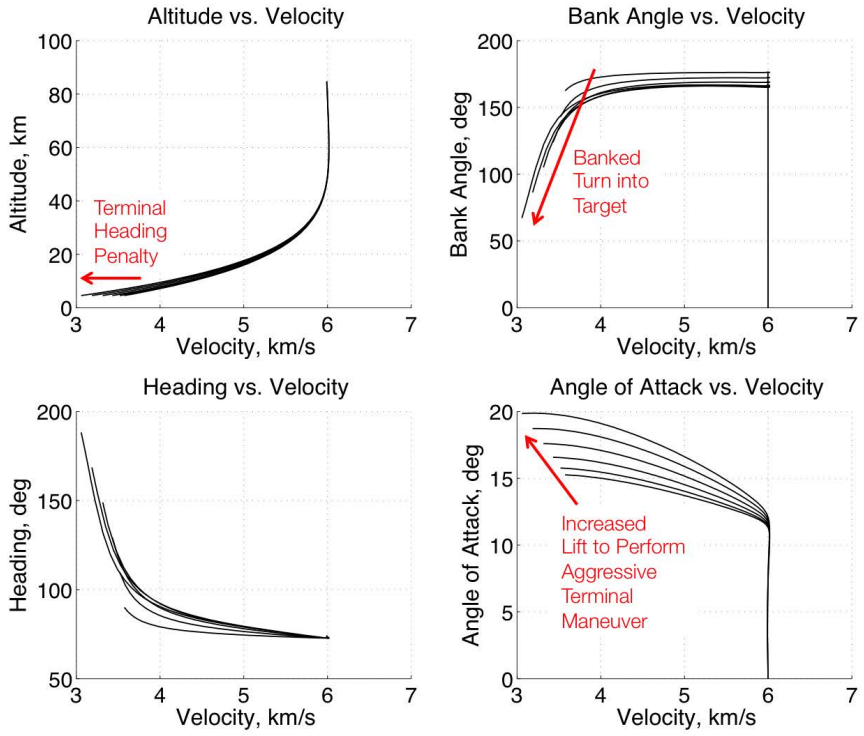

Figure 5. Trajectory and control during continuation of terminal heading.

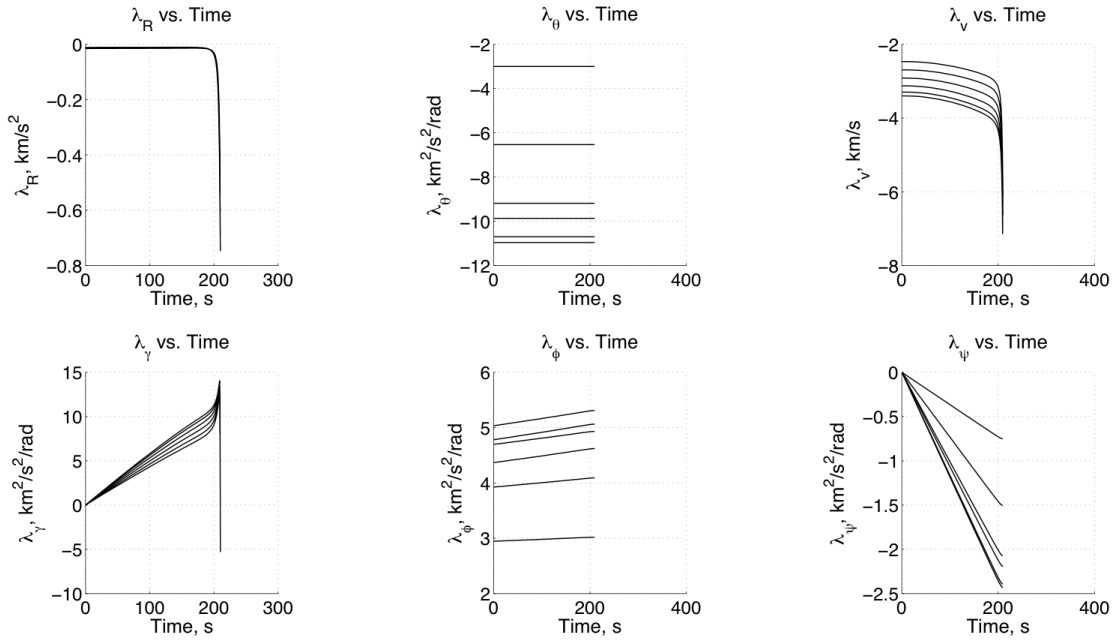

Figure 6. Costates during continuation of terminal heading.

B. Glide Body Deployment Geometry Constraints

In this example, the terminal heading is no longer constrained. Instead, a family of maximum terminal velocity trajectories is constructed for a range of initial headings as shown in Fig. 7. This example demonstrates that complex trajectories can be constructed using the rapid indirect optimization framework for any complex combination of initial and/or terminal constraints. The entire continuation process was executed in 50 seconds using the GPU. While the weapon is not launched in the direction of the target, the resulting trajectories demonstrate that it is possible to identify optimal solutions regardless of how the weapon is used. Additionally, these examples are a precursor to the enforcement of country overflight constraints in which the weapon cannot be directly launched toward the target.

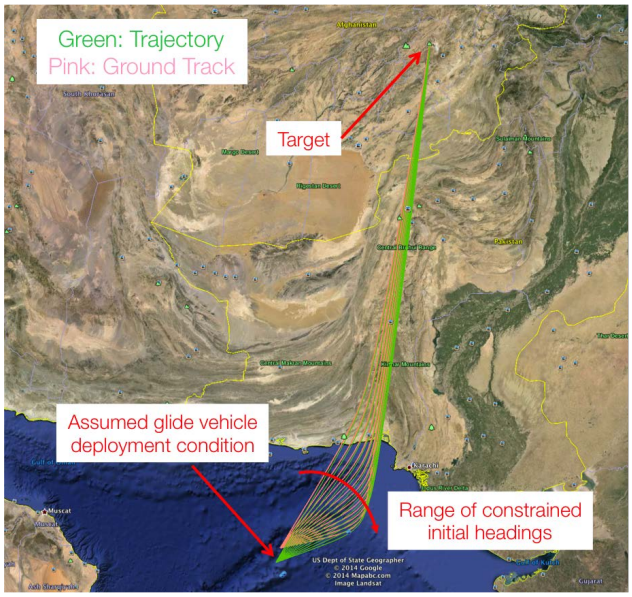

Figure 7. Overview of initial heading constrained trajectories.

The skip maneuvers required to maximize terminal velocity is shown in Figs. 8 and 9 for the same range of initial headings. As expected, initial headings directed farther away from the target require the vehicle to dive deeper into the atmosphere. This enables the vehicle to generate greater lift to perform a more aggressive turn towards the target. At the same time, this lift is also used to loft the vehicle to higher altitudes, thereby minimizing drag and maximizing velocity on target. As such, this example demonstrates that the complex trajectories constructed by the indirect optimization framework are indeed optimal. Note that the terminal azimuth costate, λ_ψ, (shown in Fig. 10) is zero as expected when the terminal heading constraint is removed. The use of detailed costate information to construct optimal solutions enables the construction of high quality, three dimensional, multi-control trajectories for aerospace problems of interest.

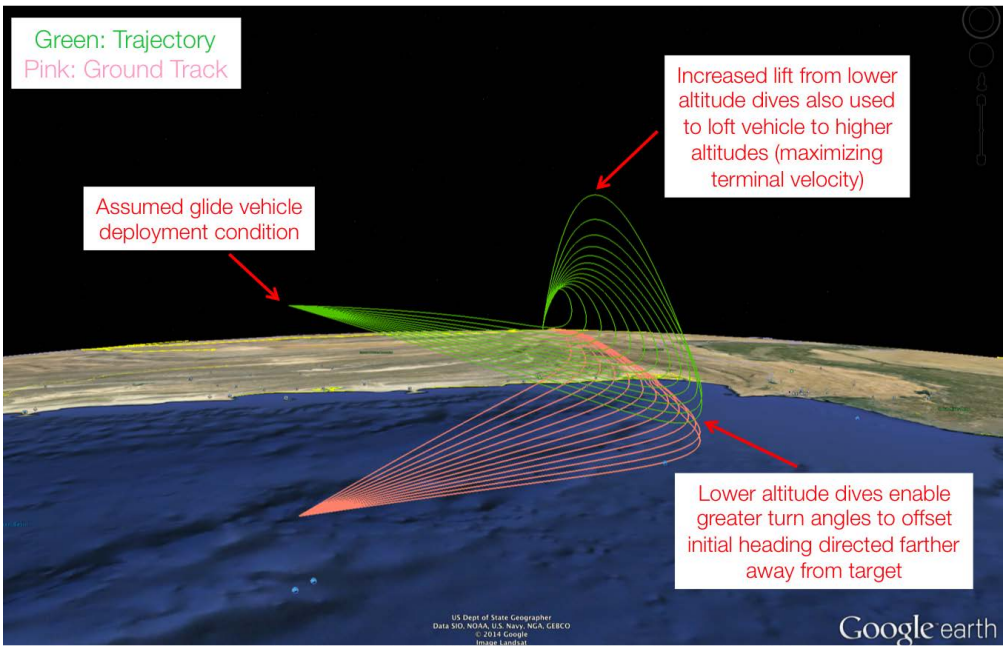

Figure 8. Dive and loft maneuver of optimal solutions.

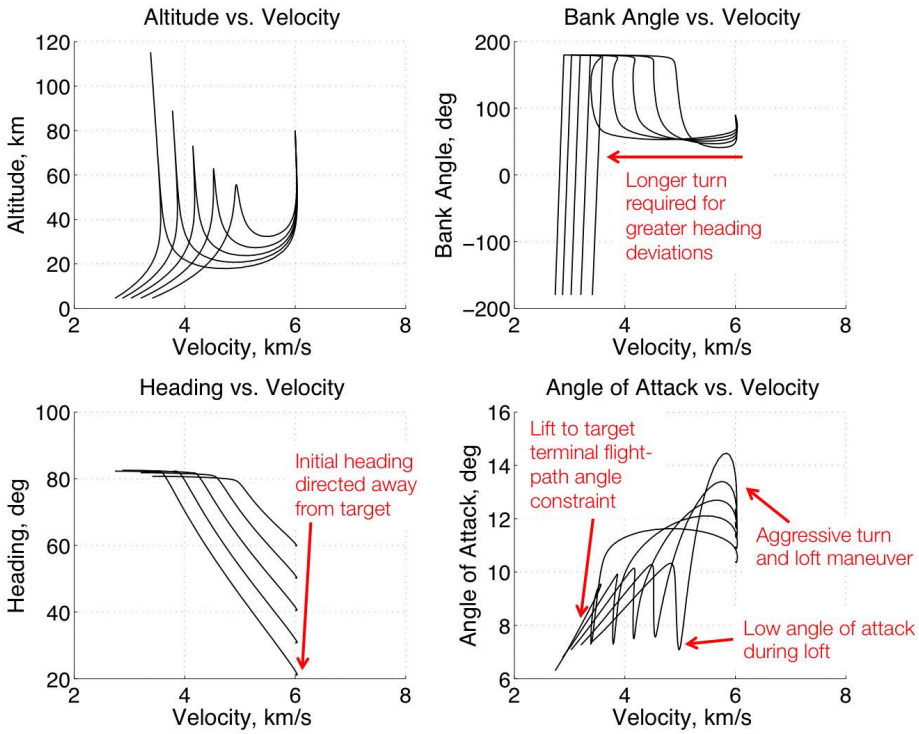

Figure 9. Trajectory and control during continuation of initial heading.

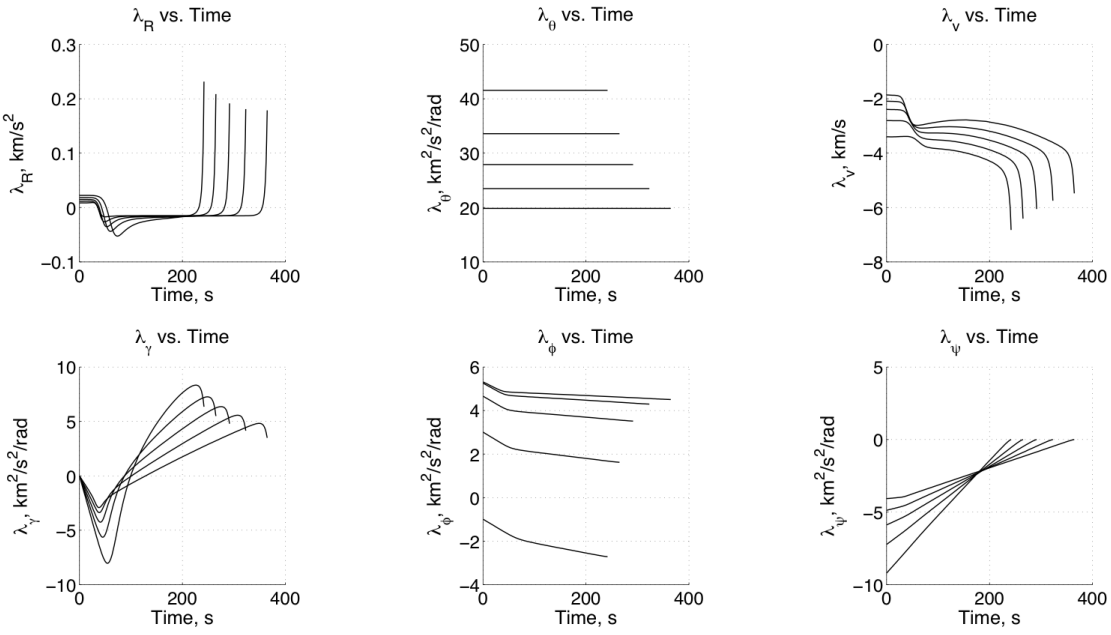

Figure 10. Costates during continuation of initial heading.

C. Stagnation Heat Rate Constraint

The prior examples demonstrated that complex trajectories can be constructed for initial and terminal constraints. In this example, a path constraint in stagnation heat rate (Eq. (12)) is added. The incorporation of this path constraint into the necessary conditions of optimality is completely automated and does not require user insight. The influence of the stagnation heat rate on the optimal solution is shown in Fig. 11. As the heat rate constraint is made more strict, the vehicle is required to fly at higher altitudes. This, in turn, reduces control authority which delays the turn to the target. During this continuation process, the heat rate constraint is incrementally (but rapidly) changed to the desired value as shown in Fig. 12. This process required 51 seconds using the GPU. As shown, the corresponding initial angles of attack are increased to ensure satisfaction of the stagnation heat rate constraint. The use of indirect methods enables the generation of high quality solutions that satisfy constraints with high precision. The corresponding costate histories are shown in Fig. 13. Since the stagnation heat rate constraint (Eq. (12)) is only an explicit function of radial magnitude and velocity, discontinuities are only observed in the corresponding costates. These corner conditions are also simultaneously solved with high precision during the solution process.

$$\dot{q} = k\sqrt{\frac{\rho}{r_n}}v^3 \leq \dot{q}_{max} \tag{12}$$

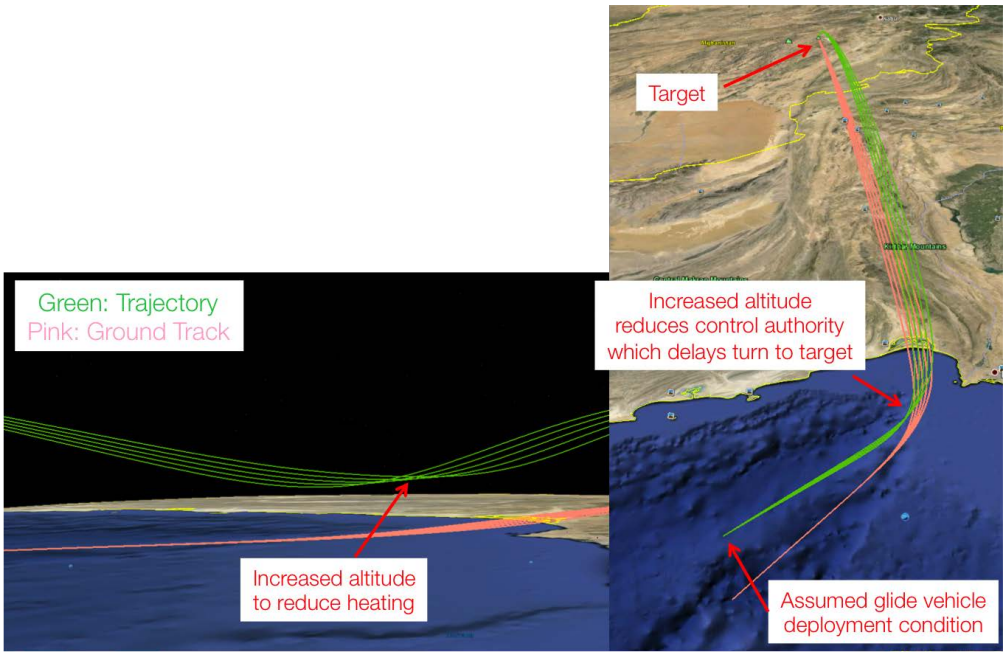

Figure 11. Increased altitude and delayed turn due to stagnation heat rate constraint.

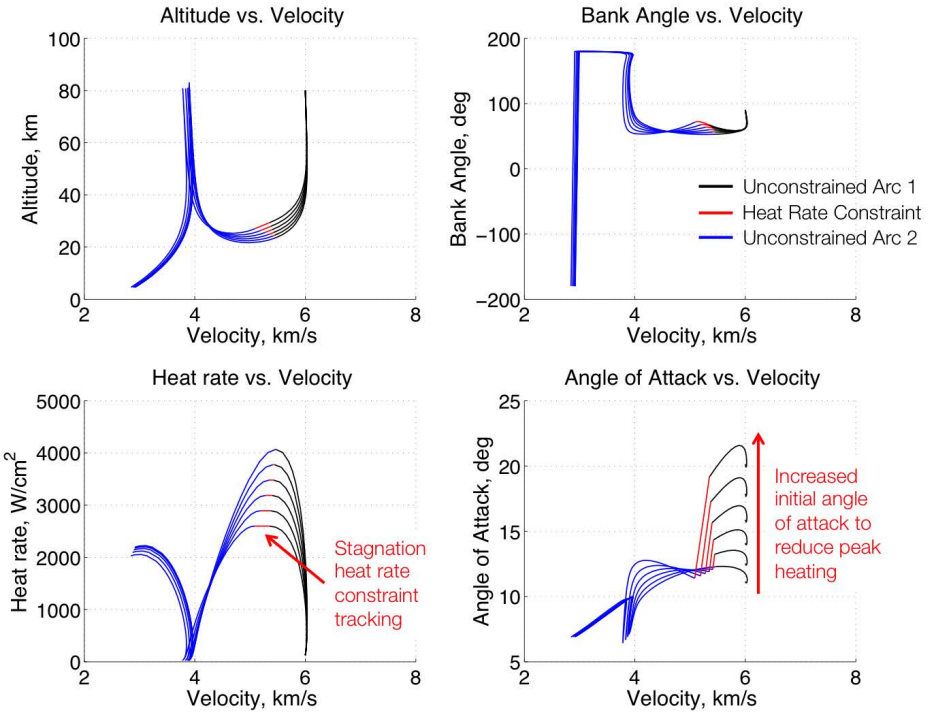

Figure 12. Trajectory and control during continuation of stagnation heat rate constraint.

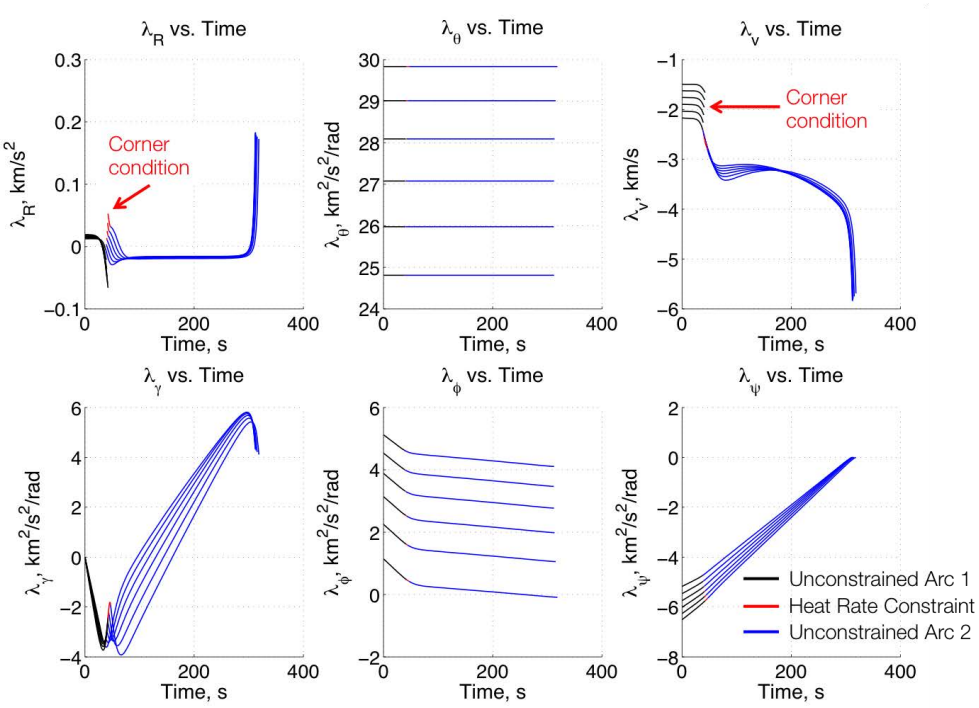

Figure 13. Costates during continuation of stagnation heat rate constraint.

D. Country Overflight Constraint

In this hypothetical example, a maximum terminal velocity trajectory is desired that does not overfly Pakistan. After a maximum terminal velocity trajectory is constructed that directly connects the glide body deployment location and target, the trajectory is "pushed" outside of Pakistan via continuation as shown in Figs. 14 and 15. This is accomplished by enforcing an interior point constraint in the form of a waypoint, and the insertion of this constraint is performed transparently to the designer. This is a required component of overflight constraints since the vehicle (with limited lift) cannot track complex border geometries. During this continuation process, the complex, simultaneous evolution of states, costates, corner conditions, control, etc. is performed rapidly with high precision in a manner that is completely transparent to the designer. This results in the construction of very high quality trajectories, and the entire process was executed in 85 seconds using the GPU. This high quality is evident in the final "corkscrew" trajectory that ensures the vehicle is capable of maximizing velocity on target while simultaneously returning to the center of the family of trajectories to satisfy the constrained terminal heading.

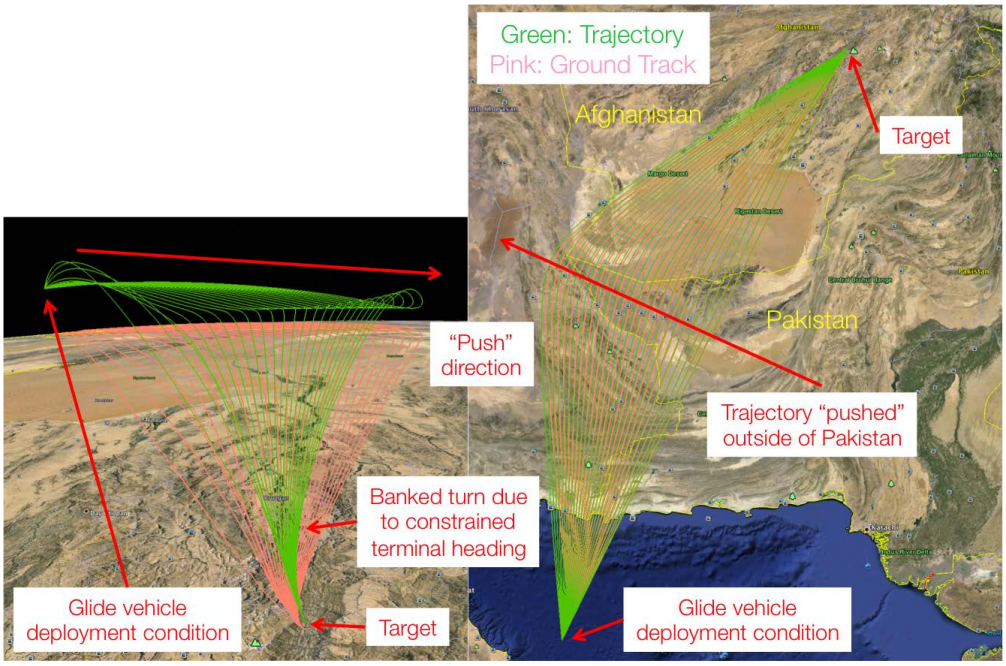

Figure 14. Example of adhering to country overflight constraint.

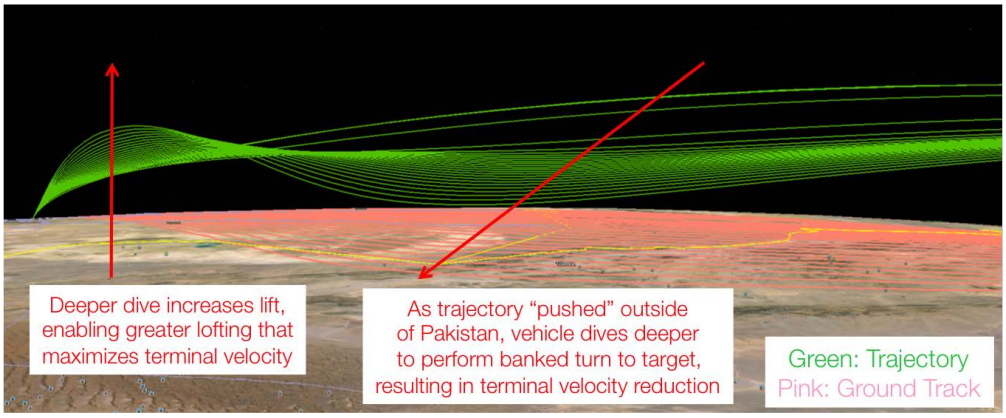

Figure 15. Turn and loft maneuver associated with country overflight constraint.

A sample of optimal solutions from this family is shown in Fig. 16 and are identified by the pre-waypoint trajectory (Unconstrained Arc 1) and post-waypoint trajectory (Unconstrained Arc 2). The transition be-

tween the arcs denotes the trajectory location of the waypoint constraint. Since the waypoint requires the vehicle to initially fly away from the target and turn toward the target at the waypoint, it is critical to ensure that the vehicle has sufficient control authority to perform this maneuver. Alternatively, the vehicle should also incorporate trajectory lofts to minimize drag, thereby maximizing velocity on target. As shown in Fig. 16, this waypoint turn is performed in the bottom portion of a loft maneuver. As such, these considerations are balanced with high precision to construct maximum terminal velocity solutions. The corresponding evolution of costates is shown in Fig. 17. Since the waypoint constraint is expressed in latitude and longitude coordinates, a corner in both latitude and longitude costates is observed at the waypoint as expected.

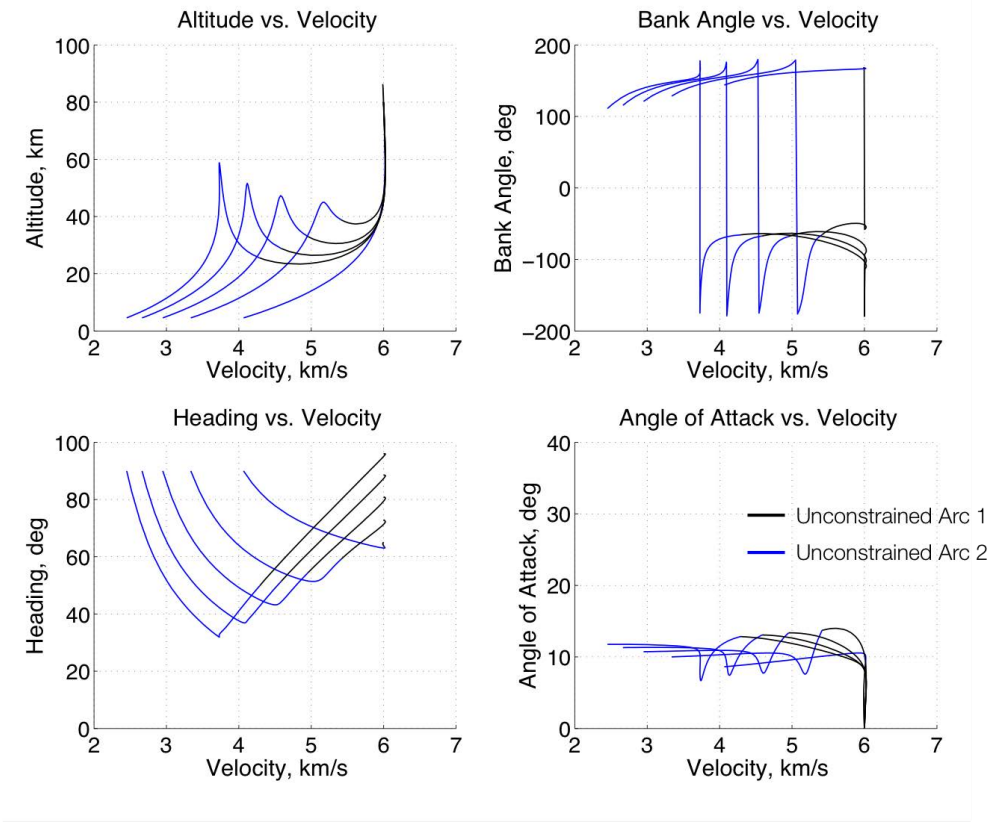

Figure 16. Trajectory and control during continuation of waypoint constraint.

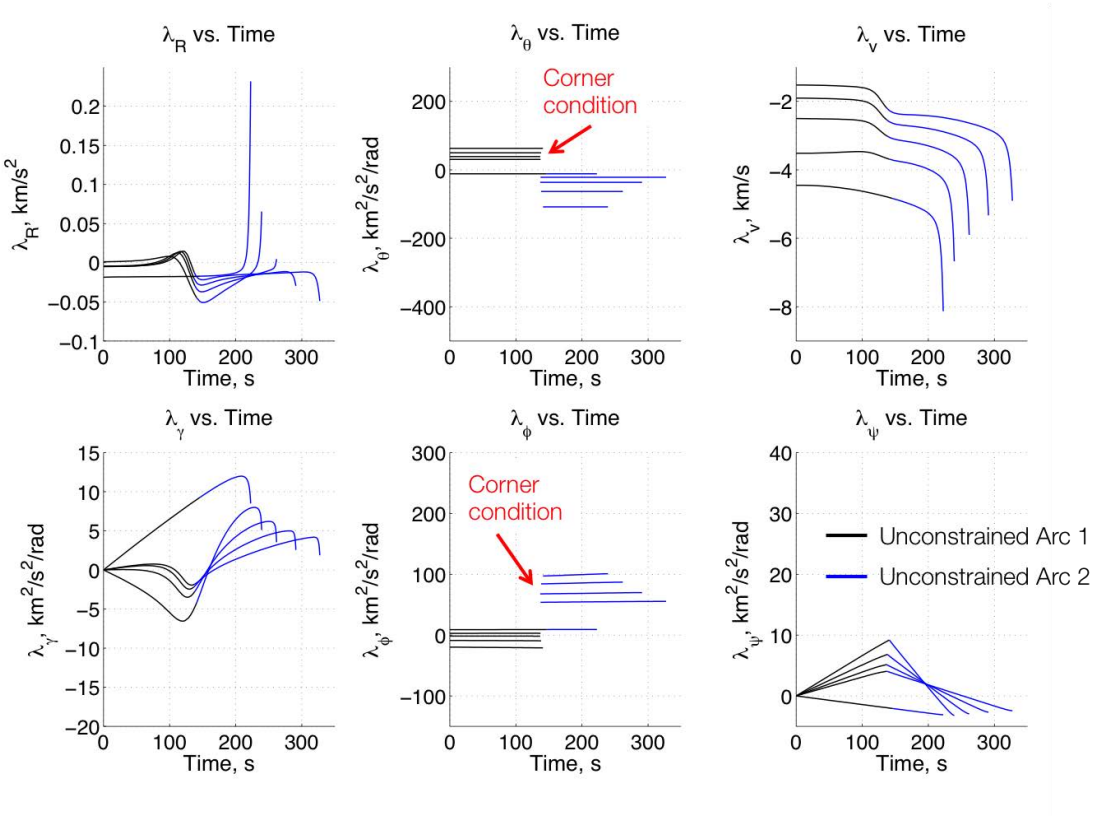

Figure 17. Costates during continuation of waypoint.

E. Combination of Constraints

The prior examples demonstrate an ability to incorporate a wide range of mission considerations and constraints. The ability to rapidly construct families of optimal solutions is particularly useful when performing trade studies. However, in many cases only the final, complex trajectory that satisfies all mission constraints is of interest. This example demonstrates that all prior constraints can be combined to construct very complex optimal trajectories using indirect optimization methods. In this hypothetical example, the weapon is initially directed toward a hypothetical target in Pakistan as shown in Fig. 18. Prior to deployment, the weapon is redesignated to a high-value target in Afghanistan. The glide body redesignated trajectory is optimized to simultaneously satisfy constraints in initial heading and velocity, stagnation heat rate, contested airspace avoidance zones, and impact flight-path angle. The optimized trajectory shown in Figs. 18 and 19 was constructed in 75 seconds using the obsolete GPU.

As shown in Fig. 18, the S-shaped trajectory requires sufficient control authority at two locations to alter the direction of the weapon's trajectory. Both of these troughs are shown in Fig. 19 in which subsequent lofts are performed during relatively straight

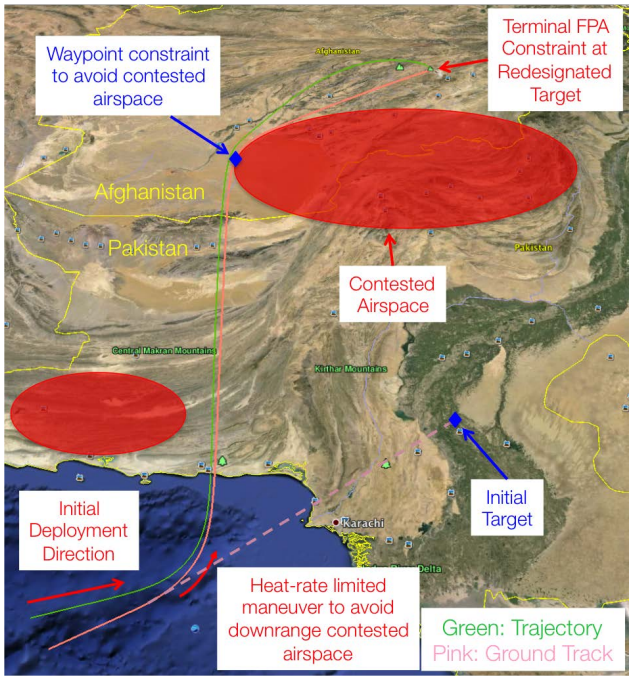

Figure 18. Overview of redesignated trajectory with multiple constraints.

portions of the trajectory to minimize the drag on the weapon. Note that the complex control histories (Fig. 19) and corner conditions (Fig. 20) associated with the entrance to the stagnation heat rate constraint and flight through the waypoint constraint are solved with high precision using the indirect methodology. The costates along the initial portion of the trajectory are emphasized in Fig. 21 to further highlight the corner conditions associated with the entrance to the heat rate constraint.

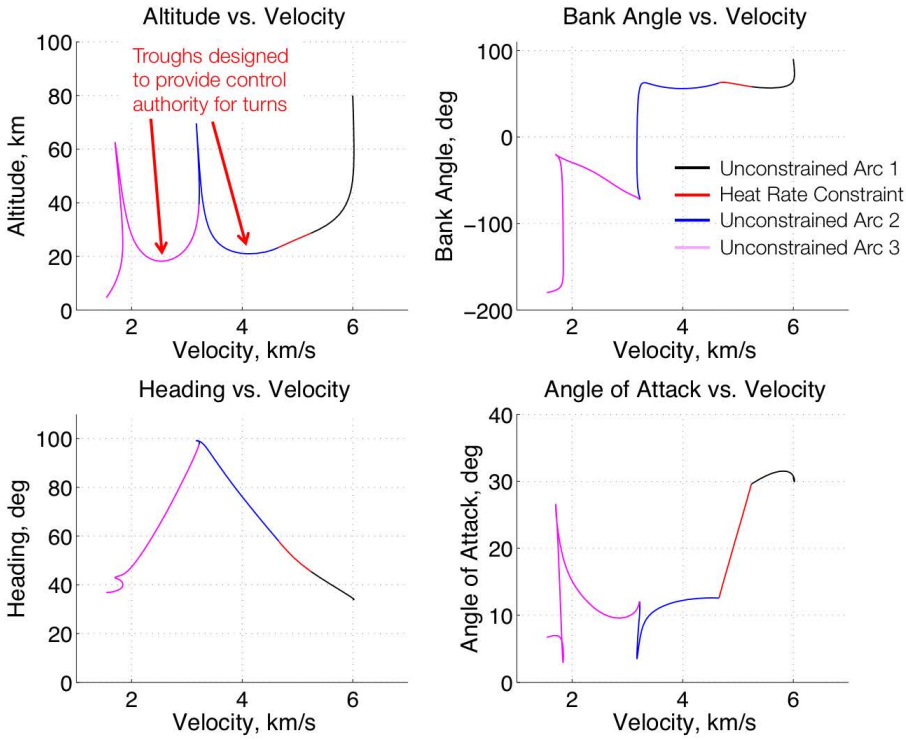

Figure 19. Trajectory and control of redesignated trajectory.

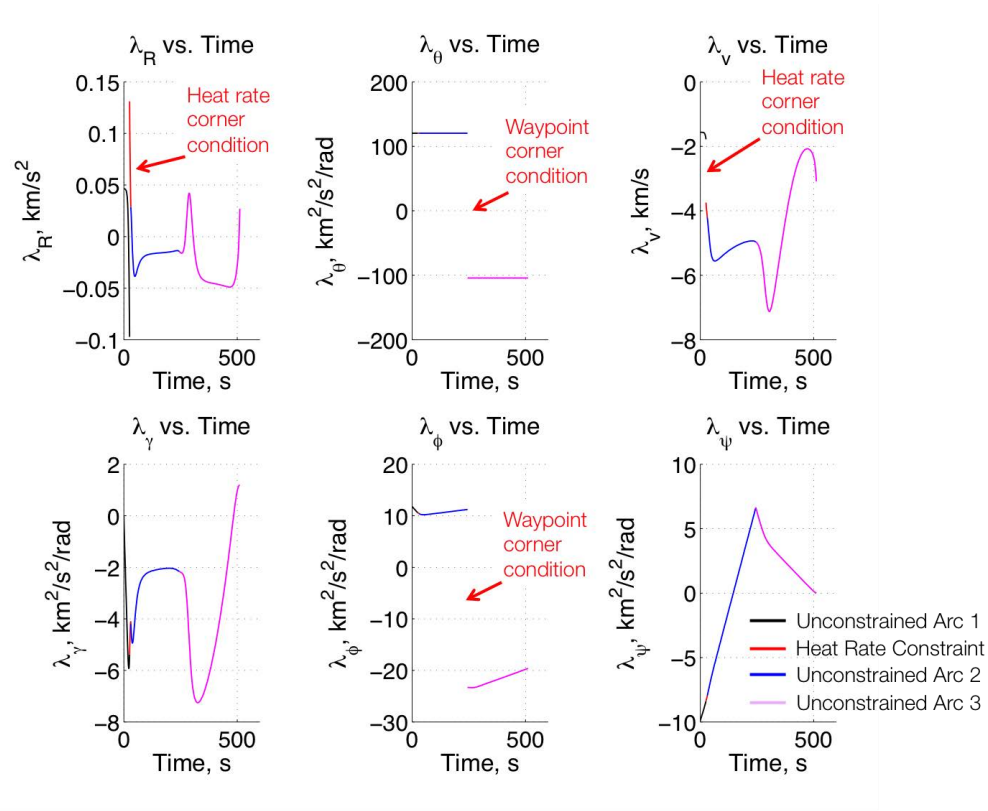

Figure 20. Costates of redesignated trajectory.

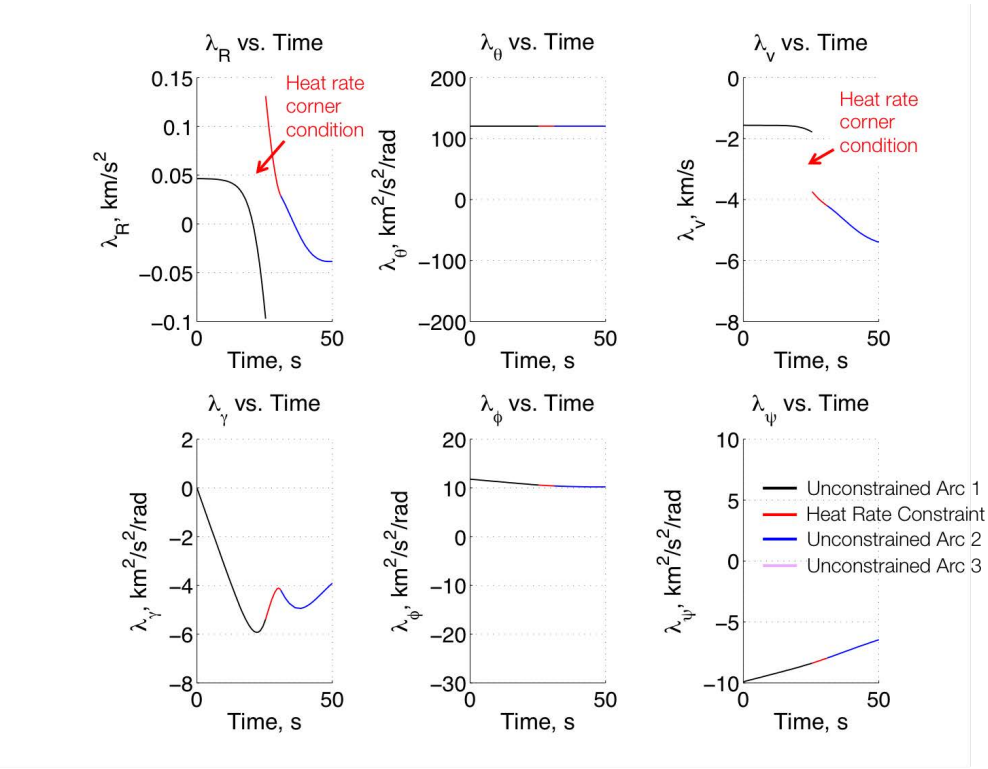

Figure 21. Costates during initial portion of redesignated trajectory.

V. Summary

In this investigation, an indirect optimization methodology is matured and applied to the design of maximum terminal velocity trajectories associated with a hypothetical long range weapon system. Examples demonstrate the ability to rapidly construct high quality indirect optimal solutions for aerospace problems of interest. Various initial, terminal, path, and interior point constraints can be enforced to support a wide range of missions of interest, and these constraints are applied in a manner that is completely transparent to the user. An initial guess for these problems is shown to be effectively constructed using an analytic ballistic trajectory solution in which the weapon is initially aimed downward. This enables rapid convergence to a maximum terminal velocity solution, and this solution is modified via continuation to satisfy an assumed set of glide body deployment conditions, impact conditions, and in-flight constraints. The necessary conditions of optimality are fully satisfied along these complex trajectory solutions, including corner conditions. These complex solutions are made possible by advancing the indirect optimization framework to support arbitrary degrees of freedom, assessment of multiple control options using Pontryagin's Minimum Principle, dynamic scaling during the continuation process, and the ability to construct a single, generic formulation of the necessary conditions of optimality to support the wide range of solutions obtained during the continuation process.

Acknowledgments

The authors would like to thank the Charles Stark Draper Laboratory for support of this research through the University Research and Development Program. The authors would like to specifically thank Roy Setterlund and David Benson for their insights and comments throughout the project.

References

[1]Lu, P. and Xue, S., "Rapid Generation of Accurate Entry Landing Footprints," *Journal of Guidance, Control, and Dynamics*, Vol. 33, No. 3, May 2010, pp. 756–767. 1

[2]Jorris, T. R. and Cobb, R. G., "Multiple Method 2-D Trajectory Optimization Satisfying Waypoints and No-Fly Zone Constraints," *Journal of Guidance, Control, and Dynamics*, Vol. 31, No. 3, May 2008, pp. 543–553. 1

[3]Jorris, T. R. and Cobb, R. G., "Three-Dimensional Trajectory Optimization Satisfying Waypoint and No-Fly Zone Constraints," *Journal of Guidance, Control, and Dynamics*, Vol. 32, No. 2, March 2009, pp. 551–572. 1

[4]Saraf, A., Leavitt, J., Ferch, M., and Mease, K., "Landing Footprint Computation for Entry Vehicles," *AIAA Guidance, Navigation, and Control Conference and Exhibit*, AIAA 2004-4774, Providence, RI, Aug. 2004. 1

[5]Fahroo, F., Doman, D. B., and Ngo, A. D., "Modeling Issues in Footprint Generation for Reusable Launch Vehicles," *2003 IEEE Aerospace*, IEEE, March 2003, pp. 2791–2799. 1

[6]Jorris, T., Schulz, C., Friedl, F., and Rao, A., "Constrained Trajectory Optimization Using Pseudospectral Methods," *AIAA Atmospheric Flight Mechanics Conference and Exhibit*, AIAA 2008-6218, Honolulu, HI, Aug. 2008. 1, 2

[7]Josselyn, S. and Ross, I. M., "Rapid Verification Method for the Trajectory Optimization of Reentry Vehicles," *Journal of Guidance, Control, and Dynamics*, Vol. 26, No. 3, May 2003, pp. 505–508. 1, 2

[8]Betts, J. T., *Practical Methods for Optimal Control and Estimation Using Nonlinear Programming*, Society for Industrial and Applied Mathematics, 2010. 1

[9]Betts, J. T., "Survey of Numerical Methods for Trajectory Optimization," *AIAA Journal of Guidance, Control, and Dynamics*, Vol. 21, No. 2, 1998. 1

[10]Jorris, T. R., Schulz, C. S., Friedl, F. R., and Rao, A. V., "Constrained Trajectory Optimization Using Pseudospectral Methods," AIAA-2008-6218, *AIAA Atmospheric Flight Mechanics Conference and Exhibit*, Honolulu, HI, 18-21 Aug. 2008. 1

[11]Bibeau, R. and Rubenstein, D., "Trajectory Optimization for a Fixed-Trim Reentry Vehicle Using Direct Collocation and Nonlinear Programming," AIAA-2000-4262, *AIAA Guidance, Navigation, and Control Conference and Exhibit*, Denver, CO, 14-17 Aug. 2000. 1

[12]Herman, A. and Conway, B., "Direct Optimization Using Collocation Based on High-Order Gauss-Lobatto Quadrature Rules," *AIAA Journal of Guidance, Control, and Dynamics*, Vol. 19, No. 3, 1996. 1

[13]Betts, J. T., *Practical Methods for Optimal Control and Estimation Using Nonlinear Programming (Second Edition)*, SIAM, Philadelphia, PA, Nov. 2010. 2

[14]Grant, M. J. and Braun, R. D., "Rapid Indirect Trajectory Optimization for Conceptual Design of Hypersonic Missions," *Journal of Spacecraft and Rockets*, Vol. 52, No. 1, Jan. 2015, pp. 177–182. 2

[15]Grant, M., *Rapid Simultaneous Hypersonic Aerodynamic and Trajectory Optimization for Conceptual Design*, Ph.D. thesis, Georgia Institute of Technology. 2

[16]Bryson, A. E. and Ho, Y.-C., *Applied Optimal Control*, Taylor and Francis, 1975. 4

[17]Elsgloc, L. D., *Calculus of Variations*, Dover Publications, Inc., 2007. 4

[18]Petrov, I. P., *Variational Methods in Optimum Control Theory*, Academic Press Inc., 1968. 4

[19]Allen, H. J. and A. J. Eggers, J., "A Study of the Motion and Aerodynamic Heating of Ballistic Missiles Entering the Earth's Atmosphere at High Supersonic Speeds," *Report 1381, National Advisory Committee for Aeronautics*. 5